doi:10.1246/cl.2010.1152
Published on the web October 5, 2010

Electrochemical Investigation of Dynamic Solution Structures of Bicontinuous Microemulsion at Solid Interfaces

Yuichi Makita,[1] Shinobu Uemura,[1] Nagayoshi Miyanari,[1] Takaaki Kotegawa,[1] Shintaro Kawano,[1] Taisei Nishimi,[2] Masato Tominaga,[1] Katsuhiko Nishiyama,[1] and Masashi Kunitake*[1,3]
[1]*Graduate School of Science and Technology, Kumamoto University, 2-39-1 Kurokami, Kumamoto 860-8555*
[2]*Frontier Core-Technology Laboratories, FUJIFILM Corporation, 210 Nakanuma, Minami-Ashigara, Kanagawa 250-0193*
[3]*Core Research for Evolutional Science and Technology (CREST), Japan Science and Technology Agency*

(Received August 20, 2010; CL-100722; E-mail: kunitake@chem.kumamoto-u.ac.jp)

Dynamic solution structure of a three-phase interface (oil/water/solid) of a bicontinuous microemulsion (BME) was evaluated electrochemically with apparent diffusion coefficients (D_{app}'s) from cyclic voltammograms. With hydrophilic (ITO) and lipophilic (pyrolytic graphite) electrodes, D_{app}'s were much smaller than with an amphiphilic (Au) electrode. The D_{app} ratios of ITO:PG-b in the BME were larger than those in a homogeneous aqueous solution. These results indicate that BME solution structures around hydrophilic and lipophilic electrodes adopt alternately layered structures but not simple sloped structures.

Bicontinuous microemulsions (BMEs) have attracted attention in various research fields because of their unique solution structures, in which the water and oil phases bicontinuously coexist on a microscopic scale.[1,2] A variety of unique nanostructure materials prepared by the polymerization or gelation of BMEs, such as continuous porous polymer materials, vertically extended nanosheet arrays and hydro/organo hybrid gels, have been reported.[3–5] BME nanostructures are also attractive as media for electrochemical studies.[6,7] Rusling et al. conducted pioneering work on the electrochemistry of BME solution with a glassy carbon electrode.[8] In our previous research we reported that electrochemical contact with the micro aqueous and organic solution phases in a BME is alternately or simultaneously achieved by controlling the hydrophilicity and lipophilicity on the electrode surfaces.[9,10] In other words, the solution structure of BME around the electrode is thermodynamically changed in response to the hydrophilic and lipophilic balance (HLB) of the electrode surfaces. A well-balanced BME solution structure is easily converted to a biased or one-sided structure on an electrode surface to minimize surface energy. Herein, we report the electrochemical investigation of liquid/liquid structures of a BME near various electrode surfaces. The unique dynamic nanostructures were elucidated from the apparent diffusion coefficients (D_{app}'s) of hydrophilic and lipophilic redox compounds in aqueous and oil phases, respectively. Furthermore, the morphologies of the BME polymerized structures in a capillary glass were determined and compared with the solution structure.

BME solutions consisting of aqueous NaCl solution, sodium dodecyl sulfate (SDS), 2-butanol, and toluene were prepared according to previous reports.[9,10] $K_3Fe(CN)_6$ and ferrocene (Nacalai Tesque Inc., Japan) were used as hydrophilic and lipophilic redox compounds, respectively, in the BME solution. Cyclic voltammograms (CVs) of the BME solutions were obtained using a PC-controlled electrochemical analyzer (ALS 814B, BAS Inc., Japan). A Pt wire and a saturated calomel electrode (SCE, BAS Inc., Japan) were also placed in the BME solution as counter and reference electrodes, respectively.[9,10] As the working electrodes, an ITO electrode, an Au disc electrode (BAS Inc., Japan), and basal plane pyrolytic graphite (PG-b, BAS Inc., Japan) were used as hydrophilic, amphiphilic, and lipophilic surfaces, respectively. Detailed information on preparation of electrodes is described in Supporting Information.[11]

Figure 1 shows typical CVs of $K_3Fe(CN)_6$ and ferrocene in the BME solution obtained with the three electrodes. The amphiphilic Au disc electrode revealed both redox peak couples for $K_3Fe(CN)_6$ and ferrocene (Figures 1B and 1E, respectively) in each BME solution. In the BME with both species, both redox peak couples are simultaneously observed.[9] In contrast, the ITO and PG-b electrodes only produced one of the peak couples of $K_3Fe(CN)_6$ or ferrocene, which have affinities for the detecting electrodes (Figures 1C and 1D). These results indicate that the BME structure is drastically changed according to the surface characteristics of the electrode.

D_{app} values for each redox species in the BME solutions were estimated from a series of CVs with different scan rates according to Randles-Ševčik equation (eq 1):[12]

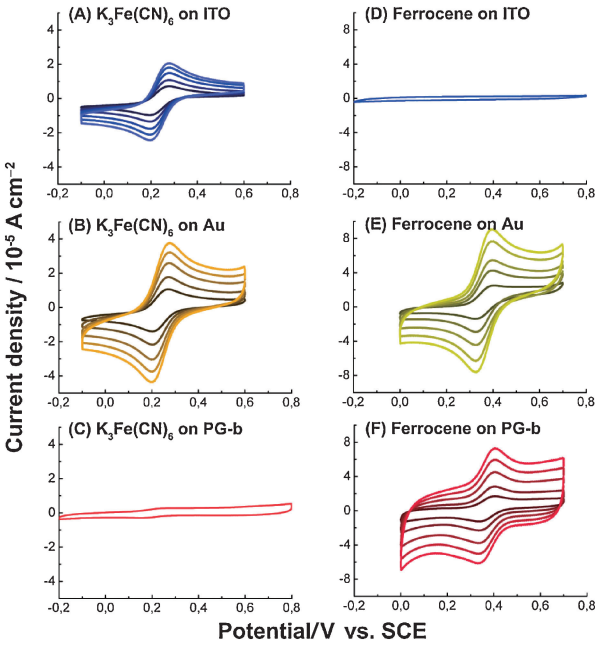

Figure 1. Typical CVs of $K_3Fe(CN)_6$ (A–C) and ferrocene (D–F) with various electrodes in the BME solution. Scan rates are 10, 25, 50, 75, and 100 mV s^{-1}.

Table 1. Apparent diffusion coefficients of ferrocene and $K_3Fe(CN)_6$ in the BME for different electrodes

	WE	$D_{app}/10^{-6}\,cm^2\,s^{-1}$		
		10 °C	20 °C	30 °C
$K_3Fe(CN)_6$ aqueous solution	Au	6.0	11	13
	ITO	7.7	11	14
$K_3Fe(CN)_6$ in BME	Au	1.9	2.6	2.8
	ITO	0.72	1.0	1.3
Ferrocene in BME	Au	2.7	6.1	8.6
	PG-b	1.2	3.2	7.6

$$i_p = 0.4463nFACD^{1/2}(nF/RT)^{1/2}v^{1/2} \quad (1)$$

where i_p is the peak current, n is the number of moles of electrons transferred in the reaction, F is the Faraday constant, A is the projected electrode area, C is the concentration of redox compound, D is the diffusion coefficient, and v is the scan rate. Therefore, D_{app} is calculated from the slope of a plot of peak current versus square root of the scan rate. The concentrations of the redox species were estimated as half of those in homogeneous media, because we used the same volume of oil and saline in the BME. Despite the complex solution structures, the linearity of plots was maintained for all systems, which provided good electrochemical response from 5 to 100 mV s^{-1} with all of the electrodes. A sigmoidal-shaped CV was not observed for all systems.

D_{app}'s obtained for each redox species with the different electrodes are summarized in Table 1. In an aqueous electrolyte solution, ITO and Au disc electrodes gave essentially the same D values for $K_3Fe(CN)_6$ at 30 °C ($D = 1.3 \times 10^{-5}\,cm^2\,s^{-1}$ at 25 °C).[13] These D values increased linearly with increasing temperature. Interestingly, the D_{app} of the Au disc electrode in the aqueous solution at 10 °C was different. Certainly, the peak separation in the CVs was not constant and increased with the increasing scan rates and low reproducibility, which is indicative of disturbance of electron transfer by surface poisoning. It is worth emphasizing that the electrochemical stability and reproducibility measured in the BME were high for all electrodes compared with those in an ordinary aqueous solution. This is probably due to the self-cleaning effect of BME.

D_{app}'s in BME solutions were smaller than D in the homogeneous solution in Table 1. Lindman and co-workers have reported that the self-diffusion coefficients of solution species in BME solutions are smaller than those in homogeneous solutions according to Fourier transform pulsed-gradient spin-echo NMR measurement.[14] In principle, D in a homogeneous solution should be independent of the type of electrode. Any deviation of D_{app} from the ideal D value provides information on the solution structure near the electrode surface and the electrode area due to contact with both phases. As we expected, D_{app}'s in the BME deviated obviously from the real D values, and were smaller than D in homogeneous solution. This is probably due to a specific solution structure preventing redox diffusion in the mixture of oil and aqueous phases.

Interestingly, the D_{app} values obtained using the hydrophilic ITO and lipophilic PG-b electrodes were less than half of those for the amphiphilic Au electrode. The ratios of D_{app} of $K_3Fe(CN)_6$ for Au against those for ITO in the BME were 2.6, 2.6, and 2.2 at 10, 20, and 30 °C, respectively. In comparison,

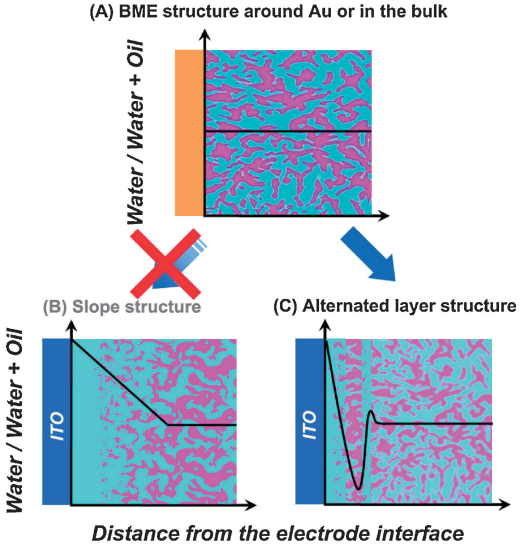

Figure 2. Schematic illustrations with depth profiles of saline volume ratio for the BME structures in bulk and amphiphilic Au electrodes (A), the slope structure (B), and alternately layered structure around hydrophilic ITO electrode (C). Magenta and light cyan regions are the oil and saline phase, respectively.

the ratios of D_{app} of ferrocene for Au against those for PG-b in the BME were 2.3, 1.9, and 1.1 at 10, 20, and 30 °C, respectively. In both cases, the ratios decreased with increasing temperature. However, the hydrophilic ITO and lipophilic PG-b electrodes consistently face either the microscopic saline phase or oil phase, respectively. The behaviors could not be explained by a simple sloped structure model as shown in Figure 2B.

The results can be explained by alternating water–oil layer structures.[15–17] The model of alternately layered structures for the hydrophilic electrode is shown in Figure 2C. The solution layers consist of microaqueous and microoil phases that form alternately starting from the electrode surface. The first solution layer is adopted because of affinity with the electrode surfaces. Next, the second counter solution layer of an oil layer or an aqueous layer forms on the aqueous or oil first layer, respectively. An alternating water–oil layer structure like this could cause the lower D_{app} values of the hydrophilic ITO and lipophilic PG-b electrodes. Compared with a bicontinuous structure (Figure 2A), the alternately layered structures would hinder diffusion of solution species (Figure 2C). Also, the contribution of the layer structure will gradually decrease with increasing distance from the electrode surface. Although the D_{app} data cannot provide information about the depth profile, the alternately layered structure model agrees with the data and characteristics of BME solutions. The ratios of D_{app}, which indicate the gap size from an ideal BME structure like a bulk solution, decreased with increasing temperature. Previously, Zhou et al. used small-angle neutron scattering to investigate the alternately layered solution structure of a BME around solid surfaces.[15–17]

Direct visual evidence of the layered structure was obtained from the surface of a BME thermal polymerization, although the thermodynamic influence from the hydrophilic/lipophilic electrode surfaces decreased with increasing temperature. On

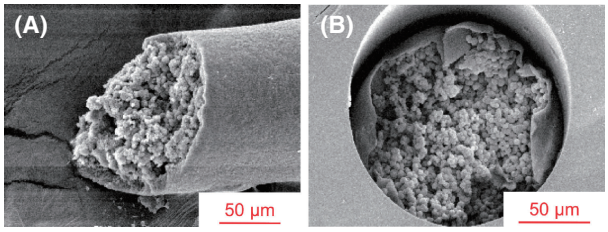

Figure 3. Typical SEM images of a polystyrene product prepared by polymerization of the BME in a hydrophilic silica capillary tube. (A) The polymerized BME taken out from a silica tube. (B) The product in a silica tube.

thermal polymerization of a BME consisting of styrene instead of toluene as the oil phase, continuous porous polystyrene products formed. The pore sizes of the products, which were kinetically changed by polymerization, were generally ten times bigger than the thickness of microaqueous phase expected in the BME. This is due to macroscopic phase separation induced by polymerization. To evaluate the influence of the surface on the solution structure of the BME, deoxidized BME was polymerized in a capillary glass, which had an intact hydrophilic surface, with azobisisobutyronitrile (AIBN) for 24 h at 60 °C. After polymerization, transparent BME solution in the capillary tube was converted into an opaque polymer. Typical cross-sectional SEM images of the polymer in the capillary tube after polymerization are shown in Figure 3. The polymer in the capillary possessed a typical continuous porous structure based on a granular network, in accordance with that observed for the bulk polymerization.[5] However, a polymer sheet (thickness $<1\,\mu m$) was also observed along the inner wall, and the porous structure based on BME was surrounded by the poreless polymer sheet. In addition, a gap between the polymer sheet and the inner wall of the capillary was frequently observed. The poreless polymer sheets might prove the existence of an alternately layered structure in BME solution before polymerization, although the wall thickness was obviously bigger than expected for microscopic oil phase before polymerization, which was due to the macroscopic phase transition induced by polymerization.

In summary, we investigated the dynamic three-phase (oil/water/substrate) nanostructures of BME around various electrodes through electrochemical techniques in terms of D_{app}. The thermodynamic structure of the BME solution near surfaces was controlled very easily by setting the conditions of BME solutions and substrates. These unique three-phase solution structures, such as sloped and alternately layered structures, have a potential as templates for development of novel polymeric materials with heterogeneous unique structures against a substrate surface.

References and Notes

1 R. Strey, *Colloid Polym. Sci.* **1994**, *272*, 1005.
2 S. P. Moulik, B. K. Paul, *Adv. Colloid Interface Sci.* **1998**, *78*, 99.
3 I. Moriguchi, Y. Katsuki, H. Yamada, T. Kudo, T. Nishimi, *Chem. Lett.* **2004**, *33*, 1102.
4 I. Moriguchi, R. Hidaka, H. Yamada, T. Kudo, H. Murakami, N. Nakashima, *Adv. Mater.* **2006**, *18*, 69.
5 S. Kawano, D. Kobayashi, S. Taguchi, M. Kunitake, T. Nishimi, *Macromolecules* **2010**, *43*, 473.
6 B. A. Marckey, J. Texter, *Electrochemistry in Colloid and Dispersions*, Wiley-VCH, New York, **1991**.
7 J. F. Rusling, *Pure Appl. Chem.* **2001**, *73*, 1895.
8 M. O. Iwunze, A. Sucheta, J. F. Rusling, *Anal. Chem.* **1990**, *62*, 644.
9 S. Yoshitake, A. Ohira, M. Tominaga, T. Nishimi, M. Sakata, C. Hirayama, M. Kunitake, *Chem. Lett.* **2002**, 360.
10 M. Kunitake, S. Murasaki, S. Yoshitake, A. Ohira, I. Taniguchi, M. Sakata, T. Nishimi, *Chem. Lett.* **2005**, *34*, 1338.
11 Supporting Information is available electronically on the CSJ-Journal Web site, http://www.csj.jp/journals/chem-lett/index.html.
12 A. J. Bard, L. R. Faulkner, *Electrochemical Methods: Fundamentals and Applications*, Wiley-VCH, New York, **1980**.
13 Y. Iwasawa, *Handbook of Chemistry (Kagaku Binran)*, Maruzen Co., Ltd., Tokyo, **2004**, p. II-45.
14 P. Guéring, B. Lindman, *Langmuir* **1985**, *1*, 464.
15 X.-L. Zhou, L.-T. Lee, S.-H. Chen, R. Stray, *Phys. Rev. A* **1992**, *46*, 6479.
16 X.-L. Zhou, S.-H. Chen, *Phys. Rep.* **1995**, *257*, 223.
17 U. Olsson, in *Handbook of Applied Surface and Colloid Chemistry*, ed. by K. Holmberg, John Wiley & Sons, **2001**, Vol. 2, Chap. 17, pp. 333–356.

